Chemistry & Biology, Vol. 11, 855–863, June, 2004, ©2004 Elsevier Ltd. All rights reserved. DOI 10.1016/j.chembiol.2004.04.011

New Addresses on an Addressable Virus Nanoblock: Uniquely Reactive Lys Residues on Cowpea Mosaic Virus

Anju Chatterji,[1] Wendy F. Ochoa, Melissa Paine,[1] B.R. Ratna,[2] John E. Johnson,[1,*] and Tianwei Lin[1,*]
[1]Department of Molecular Biology
Center for Integrative Molecular Biosciences
The Scripps Research Institute
10550 N. Torrey Pines Road
La Jolla, California 92037
[2]Center for Bio/Molecular Sciences and Engineering
4555 Overlook Avenue SW
Naval Research Laboratory
Washington, D.C. 20375

Summary

Cowpea mosaic virus (CPMV) is a robust, icosahedrally symmetric platform successfully used for attaching a variety of molecular substrates including proteins, fluorescent labels, and metals. The symmetric distribution and high local concentration of the attached molecules generates novel properties for the 30 nm particles. We report new CPMV reagent particles generated by systematic replacement of surface lysines with arginine residues. The relative reactivity of each lysine on the native particle was determined, and the two most reactive lysine residues were then created as single attachment sites by replacing all other lysines with arginine residues. Structural analysis of gold derivatization not only corroborated the specific reactivity of these unique lysine residues but also demonstrated their dramatically different presentation environment. Combined with site-directed cystine mutations, it is now possible to uniquely double label CPMV, expanding its use as an addressable nanoblock.

Introduction

Cowpea mosaic virus (CPMV) is a Picorna-like, icosahedral plant virus with a single-stranded, positive sense RNA genome and is about 30 nm in size [1, 2]. The virus can be readily purified in large quantities from common black eye pea plants [3]. Its capsid is formed by 60 copies of an asymmetric unit comprised of a small (S) and a large (L) subunit. The S subunit folds into one jelly roll β sandwich domain, the A domain, and these cluster around 5-fold axes. The L subunit is a single polypeptide chain that folds into two jelly roll β sandwich domains, B and C domains, which alternate around the 3-fold axes (Figure 1) [4]. The two RNA molecules of the genome are separately encapsidated in different isometric particles that can be separated in sucrose or CsCl gradients by ultracentrifugation [4]. The infectious cDNA clones of the virus are made under the control of the 35S promoter from Cauliflower mosaic virus for efficient and convenient transfection [5], which enables the surface properties of the capsid proteins to be altered with oligonucleotide-directed mutagenesis. The virus system has been exploited as scaffolds for chemistry, biomaterials, and functional display of ligands by bioconjugation [6–9]. Previously, unique Cys residues were introduced on the surface, and the virus particles with engineered sulfhydryls were demonstrated to be chemically reactive with well-established thiol chemistry [10]. The reactivity of the surface amines of Lys side chains was also investigated. It was shown that, among the five unique Lys residues in each of the asymmetric units, the equivalent of four amine groups could be labeled. Interestingly, one Lys in the S subunit, Lys138, seemed to be uniquely labeled under selected conditions [11]. However, as is shown in current study, the previous data were not definitive, and there is measurable reactivity for all of the Lys residues on the surface. Here, we report the systematic investigation of the amine reactivity by employing a series of Lys-minus CPMV mutants. It is demonstrated that all of the native surface amines are reactive, but to different degrees. The creation of a collection of CPMV mutants with uniquely reactive Lys side chains enriches the repertoire of addressable virus particles as nano building blocks.

*Correspondence: jackj@scripps.edu (J.E.J.); twlin@scripps.edu (T.L.)

Results and Discussion

Quality Control

Biological molecules are inherently fragile and variations in CPMV have occasionally been observed from different preparations and after extended storage. Thus, it is critical to establish the stability and chemical reactivity of all mutants in a consistent manner. Several procedures were implemented to establish criteria for judging the quality of the mutated and purified viruses (Figure 2), and these are first described in general terms and then for specific Lys-minus mutants. The integrity of the virus particles was examined by sedimentation velocity centrifugation and gel filtration chromatography. The two RNA molecules of the virus are separately encapsidated in different isometric particles. On sucrose gradients after ultracentrifugation, typically two major bands were discerned, with the bottom band corresponding to virus particles with larger RNA, RNA1, and the upper band corresponding to particles with the smaller RNA2 (Figure 2A). With excess loading, another fainter band close to the top of the gradient can also be detected, which correspond to the empty capsids. Purity of the preparation was verified by SDS PAGE (Figure 2B). The electrostatic properties of the virus particles were tested by ion exchange chromatography, and pure virus preparations showed a single peak in the chromatograms (Figure 2C). The intact virus particles were eluted in chromatography as a single peak close to the void volume on a Superose6 column (Amersham Pharmacia Biotech) (Figure 2D). The samples were also routinely stained with uranyl acetate and inspected by transmission electron microscopy (Figure 2E). Each individual procedure is not sufficient

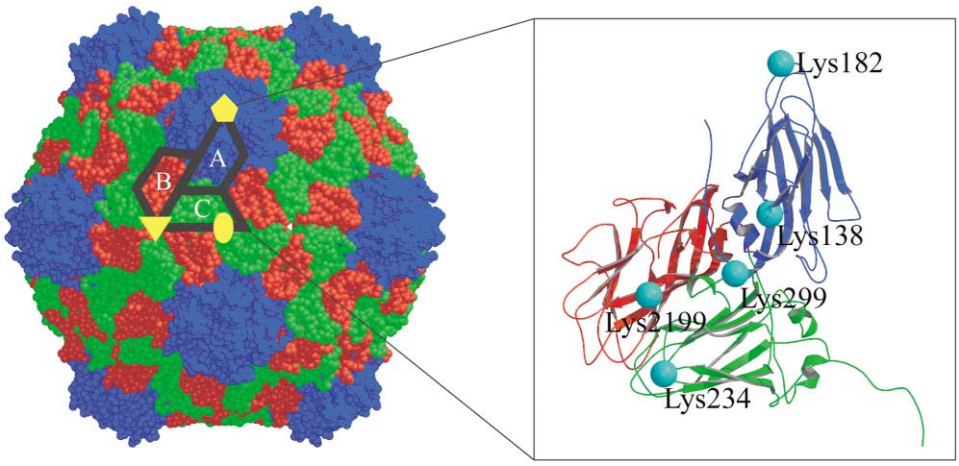

Figure 1. The Structure of the Viral Capsid and the Icosahedral Assymetric Unit of CPMV

On the left is a space-filling model of CPMV capsid. The reference asymmetric unit is framed, and the symmetry elements are labeled. Small (S) subunits labeled A are in blue, and the large (L) subunits formed by two domains are in red (B domains) and in green (C domains). The oval represents a 2-fold axis, the triangle is a 3-fold axis, and the pentagon a 5-fold axis. Shown on the right is a ribbon diagram of the asymmetric unit comprised of three jelly roll β sandwiches, with surface Lys residues represented as spheres in cyan. Residue numbers are preceded by a 1 if they are in the small subunit and a 2 if they are in the large subunit. Lys138 (residue #38) and Lys182 (residue #82) are in the A domain, Lys299 and Lys234 are in the C domain, and Lys2199 is in the B domain. The figure was drawn with MOLSCRIPT [14].

to judge the quality of the preparation. However, a combination of all the procedures collectively ensures the quality of the sample. More than 100 preparations of CPMV, employed for a broad spectrum of applications, have been tested with these criteria, and those that pass invariably result in consistent stability and chemical reactivity.

Mutagenesis and Propagation of the Mutants

There are five surface Lys residues in each CPMV asymmetric unit (Figure 1). Oligonucleotide-directed mutagenesis was employed to mutate them to Arg residues to generate Lys-minus mutants. Since the pKa of Arg residues is greater than 12, the guanidine groups are expected to be mostly protonated at pH 7, the pH at which the reactions are conducted. The protonated guanidine groups of Arg residues are poor nucleophiles and unlikely to engage in the addition reactions with NHS ester and isothiocyanate groups. The polarity and positive charge of Arg side chains, however, are likely to preserve the environment of the original Lys residues [12]. Table 1 lists the mutants generated for this investigation.

Alteration of the surface Lys to Arg residues did not interfere with the propagation of the viruses and all of the mutants' induced systemic infection in black eye peas. Total RNA extracted from both the primary and secondary leaves was examined for evidence of viral replication and genetic stability. No reversion to the wild-type viral sequence was detected by RT-PCR and DNA sequencing after five or more generations of passage. The yields of different mutants were comparable to that of the wild-type virus (Table 1). Fractionation of the Lys-minus mutants showed no alteration from wild-type virus in their banding pattern on a 10%–40% sucrose gradient by sedimentation velocity centrifugation, indicating that the particles were intact and stable. The SDS PAGE and chromatographic analysis of the purified virus did not reveal any significant differences from the wild-type virus, confirming that the mutations had not caused any major alterations in the properties of the virus.

Lys Reactivity Derived from Single Lys-Minus Mutants

The reactivity of the Lys-minus mutants was investigated by quantifying the absorbance at 495 nm of the attached fluorescein molecules after labeling the virus with NHS ester or isothiocyanate derivative of fluorescien (Figure 3A). Under slightly modified conditions from those previous employed [11], a loading of 1 to 1.3 fluorescein molecules per asymmetric unit of the native virus was consistently achieved with fluorescein isothiocyanate (FITC) and fluorescein NHS ester. There was no indication of virus disintegration or aggregation during the reaction, as judged by sedimentation velocity centrifugation and chromatography.

Mutation of single Lys to Arg residues reduced the reactivity in each of the five cases, but none of the mutations abolished the reactivity completely (Figure 3). In labeling reactions with FITC, the mutation of Lys138 to Arg residue resulted in a reduction of about 37% of the reactivity, suggesting that Lys138 was associated with significant reactivity but not as the only reactive Lys residue, as was previously reported [11]. Another significant reduction in the reactivity, about 26%, was observed as a result of mutation of Lys299 to Arg. Overall, Lys138 and Lys299 accounted for 2/3 of the total reactivity in the native virus, while the other residues, Lys182, Lys234, and Lys2199, shared roughly 1/3 of the remaining amine reactivity (Figures 3B, 3D, and Table 2). The derived reactivity from the five single Lys-minus mutants could account for almost all the reactivity (93.1%) of the wild-type virus, indicating that the reac-

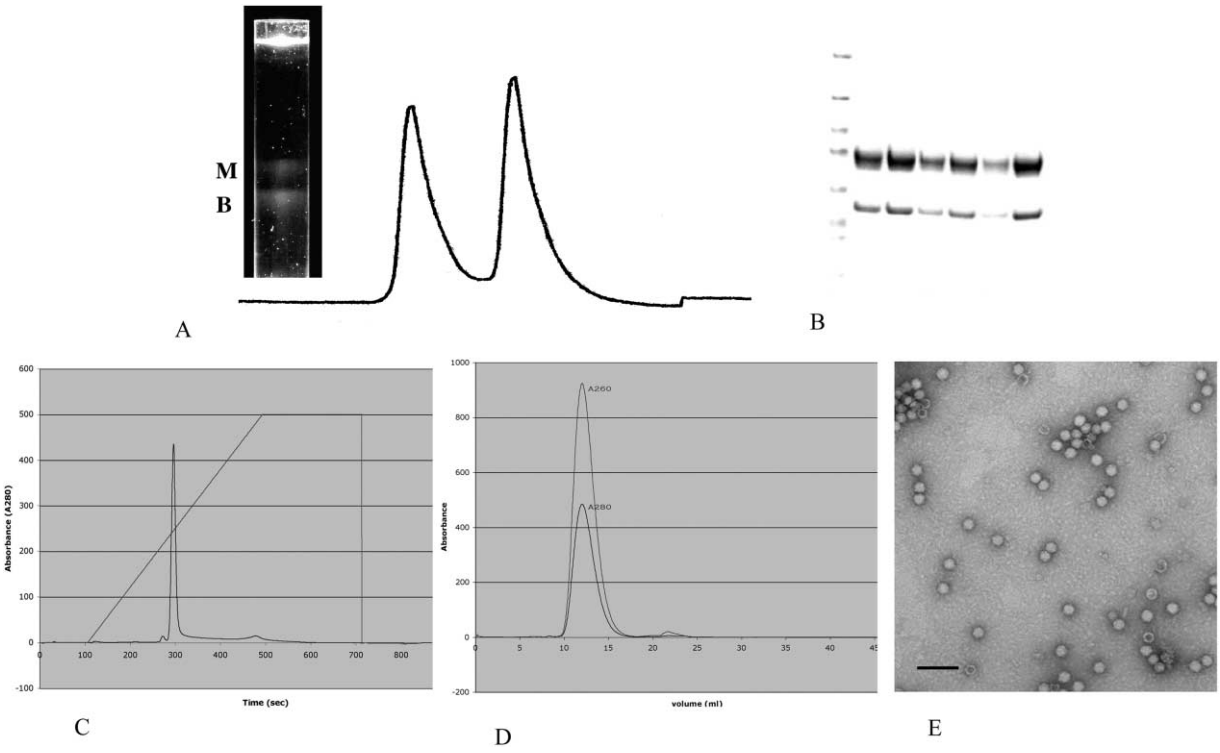

Figure 2. Quality of CPMV and CPMV Mutants

(A) Fractionation of CPMV (vK299) mutant on a sucrose gradient (10%–40%) (inset) after ultracentrifugation. The two peaks represent the middle (M) and the bottom (B) components of the virus particles. The B component (peak2) contains the larger RNA (RNA1) and has higher density, and M component (peak1) encapsidates the smaller RNA2. A peak close to the top of the gradient corresponding to the top component (empty capsids) is not visible.

(B) SDS-PAGE analysis of Lys-minus mutants of CPMV. The two subunits of the virus capsid migrate with apparent molecular weights of 23 and 38 kDa on a 4%–12% Bis-Tris (MES-SDS) NuPAGE gel (Invitrogen).

(C) Anion exchange chromatogram of a Lys-minus mutant on a monoQ column (Amersham Pharmacia Biotech) eluted against a salt gradient (1 M NaCl). Virus preparations with high quality show a single dominant peak. The x axis represents the retention time on the column in seconds, while the y axis denotes the UV absorbance measured at 280 nm.

(D) Size-exclusion chromatogram of Lys-minus mutants of CPMV eluted from a Superose6 (HR 10/10) column (Amersham Pharmacia Biotech). The homogenous preparation shows a single peak close to but not at the void volume. The aggregated virus samples elute at void volume, while disrupted particles elute off much later, corresponding to smaller molecular weight products. The x axis represents the retention volume on the column in milliliters, while the y axis denotes the UV absorbance monitored at 280 nm.

(E) TEM images of a purified preparation of Lys-minus mutant showing intact particles. The samples were stained with 0.2% uranyl acetate, and the images were acquired with a Philips Tecnai (100 Kv) electron microscope. The bar represents 100 nm.

tion was virtually specific for the Nϵ amines of the five surface Lys residues and each of the lysine residues reacted independently.

Labeling the wild-type CPMV and the Lys-minus mutants with fluorescein NHS ester resulted in more extensive labeling of each residue. However, the reactions followed similar trends as those with FITC, demonstrating that all surface Lys residues contributed to the reac-

Table 1. Lys-Minus CPMV

Virus	Mutations	Yield (mg/g of Leaves)
Wild-type		1–1.5
vK182.K234.K299.K2199	K138R	1–1.5
vK138.K234.K299.K2199	K182R	0.4
vK138.K182.K299.K2199	K234R	1–1.5
vK138.K182.K234.K2199	K299R	1–1.5
vK138.K182.K234.K299	K2199R	1–1.5
vK182.K234.K2199	K138R/K299R	0.6
vK138.K182.K2199	K234R/K299R	1–1.5
vK234.K299	K138R/K182R/K2199R	0.8
vK138	K182R/K234R/K299R/K2199R	1–1.5
vK299	K138R/K182R/K234R/K2199R	0.5
vK2199	K138R/K182R/K234R/K299R	0.8

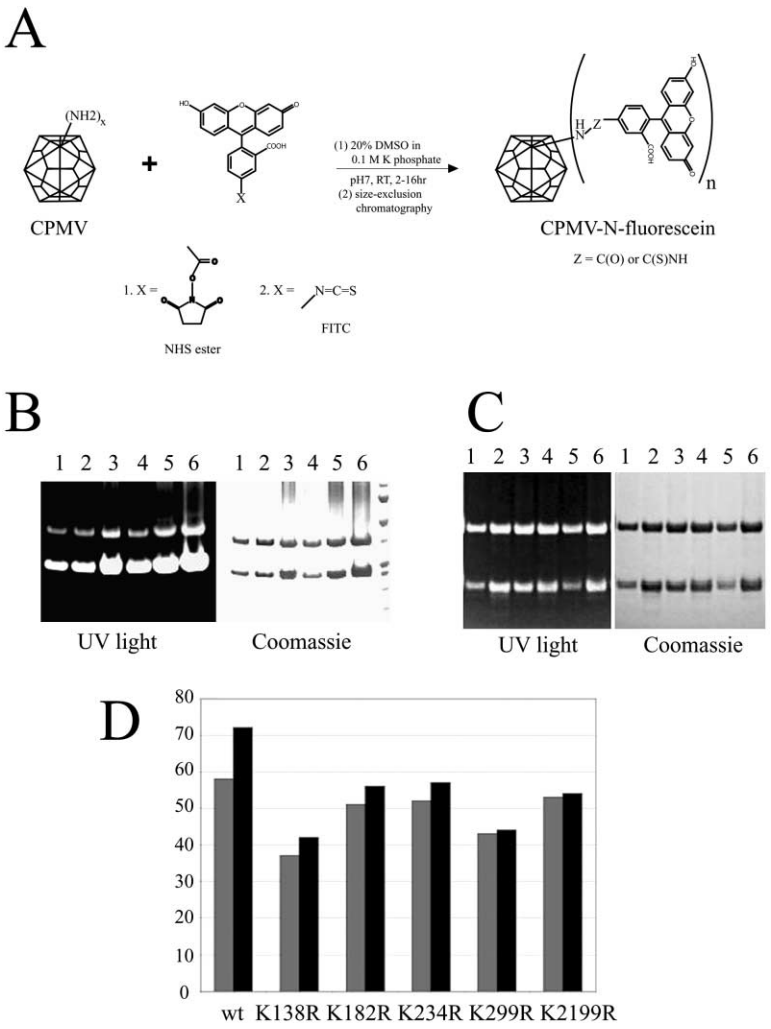

Figure 3. Quantification of Fluorescein Molecules Attached to CPMV

(A) Reaction scheme for the attachment of fluorescein to amine groups of Lys residues by FITC and NHS ester derivatives.

(B) SDS-PAGE analysis of FITC-labeled single Lys-minus mutants of CPMV under UV light (left) and stained with Coomassie Brilliant Blue (right). Lanes 1–6: K138R, K182R, K234R, K299R, K2199R, and WT CPMV.

(C) SDS-PAGE of single Lys-minus mutants labeled with fluorescein NHS ester under UV (left) and by Coomassie staining (right). Lanes 1–6: K138R, K182R, K234R, K299R, K2199R, and WT CPMV.

(D) Reduction in labeling of single Lys-minus mutants. The columns in black show the number of fluorescein molecules attached to the virus particles labeled with NHS ester, while the columns in gray denote FITC-derived virus particles. The virus mutants used in the experiment are indicated. All reactions with NHS ester were carried out at pH 7.0 at room temperature for 2 hr with 200× excess dye reactants. The reactions with FITC were carried out under similar conditions but with larger excess of dye molecules (1000×) and an extension of reaction time to 18–24 hr.

tivity (Figures 3C, 3D, and Table 2). The derived reactivity from Lys-minus mutants still accounted for 90% of the wild-type reactivity, indicating that NHS esters were associated with reasonable specificity toward Nϵ amines of Lys residues under the conditions employed. The higher loading of dye molecules by fluorescein NHS

Table 2. Labeling of CPMV Using Fluorescein NHS Ester and FITC

Virus (Mutation)	No. of Dyes/Particle (NHS Ester)	No. of Dyes/Particle (FITC)	Remaining Reactivity[a] (FITC)	Reduction in Reactivity[b] (FITC)
Wild-type	72	58		
vK182.K234.K299.K2199 (K138R)	46	37	63.8%	36.2%
vK138.K234.K299.K2199 (K182R)	60	51	87.9%	12.1%
vK138.K182.K299.K2199 (K234R)	64	52	89.7%	10.3%
vK138.K182.K234.K2199 (K299R)	53	43	74.1%	25.9%
vK138.K182.K234.K299 (K2199R)	59	53	91.4%	8.6%
vK182.K234.K2199 (K138R/K299R)	32	24	41.4%	58.6%
vK138.K182.K2199 (K234R/K299R)	48	44	75.9%	24.1%
vK234.K299 (K138R/K182R/K2199R)	34	23	39.7%	60.3%
vK138 (K182R/K234R/K299R/K2199R)	26	23	39.6%	60.4%
vK299 (K138R/K182R/K234R/K2199R)	31	24	41.4%	58.6%
vK138[c]	183	68		
vK299[c]	185	64		

[a] $\text{Reactivity}_{\text{mutant}}/\text{reactivity}_{\text{wild-type}} \times 100\%$.

[b] $(\text{Reactivity}_{\text{wild-type}} - \text{reactivity}_{\text{mutant}})/\text{reactivity}_{\text{wild-type}} \times 100\%$, which is the derived reactivity of the mutated Lys of wild-type.

[c] Dye labeling under "forcing conditions."

ester probably resulted from labeling of additional Lys residues. Since FITC appeared to be associated with better specificity toward Lys residues, it was our reagent of choice for most of the subsequent experiments in this study.

Chemical Reactivity of Double and Triple Lys-Minus Mutants

Virus particles with two or three Lys mutated to Arg residues were also generated and derivatized with FITC. The change in reactivity due to the multiple mutations was additive when compared to that of virus particles with single Lys mutations (Table 2). The reduction in reactivity due to triple mutation of K138R/K182R/K2199R was the sum of reduction in reactivity from three individual single Lys mutations of K138R, K182R, and K2199R, with an error of 7%. Similarly, the reduction in reactivity due to double mutation of K138R/K299R equaled the combined reduction of reactivity of two single Lys mutations of K138R and K299R, with an error of 6%. The higher than normal error of 30% reduction of reactivity was observed with the double mutant K234R/K299R when compared to the combined reduction in reactivity of single K234R and K299R mutations. Judging from all the data, this is likely due to the error in measurement rather than nonadditivity in reactivity. The combined reactivity of vK138.K182.K2199 and vK234.vK299, which together contained the complementary five Lys residues of the wild-type, was similar to that found in the wild-type virus within the error of 15% (Table 2).

Derivation of Quadruple Lys-Minus Mutants

Successive mutations resulted in virus particles with different combinations of Lys residues. Two mutants, vK138 and vK299, contain single reactive lysine residues, Lys138 and Lys299. Labeling experiments showed that the reactivity of these mutants was also additive with other mutants (Table 2). The combined reactivity of vK138 and vK182.K234.K299.K2199, as well as the combined reactivity of vK299 and vK138.K182.K234.2199, was summed to the reactivity of the wild-type virus (Figure 4A and Table 2). Similarly, the combined reactivity of vK138, vK299, and vK182.K234.K2199 reflected the reactivity of the wild-type virus (Figure 4A and Table 2). All of these results demonstrated that the reactivity of individual Lys residues was additive, and the amine reactivity on CPMV particles was mainly derived from the five Lys residues on the exterior surface of the virus capsid.

Complete Derivatization of Surface Lys Residues

The conditions described above for chemical derivatization of mutant virus particles did not result in complete loading of fluorescein molecules, indicating that not all of the available Lys residues on CPMV surface were modified. To demonstrate that icosahedrally equivalent Lys residues were equally addressable, mutants with single unique Lys residues were derivatized with FITC under forcing conditions (Experimental Procedures). Sixty-eight and sixty-four fluorescein molecules were attached to vK138 and vK299, respectively, indicating that all 60 equivalent Lys residues on the virus surface were labeled (Figure 4A and Table 2). However, under similar conditions there appeared to be excess loading of dye molecules with NHS esters on the same mutants (Table 2). The excess attachment by fluorescein NHS ester probably resulted from nonspecific labeling of histidines and other residues [12] or from labeling of amines in the capsid interior.

Derivatization of Unique Lysine Mutants with NANOGOLD

Two mutants of CPMV with uniquely reactive lysine residues in small (vK138) and large (vK299) subunits were treated with monosulfo NHS NANOGOLD (Nanoprobes, Inc.) to generate site-specific, metal-decorated virus particles. The CPMV/gold conjugates displayed absorbance at 420 nm, indicating the presence of gold in association with the virus particles. Structural analysis of the conjugates by cryo electron microscopy and image reconstruction showed specific labeling of the targeted lysine residues, as the electron densities corresponding to the gold particles were only associated with the unique lysine residues (Figure 4B). The striking difference in the presentation of the gold label on the two mutants suggested that the local environment of the targeted lysine residue might influence the presentation of the attached ligand. The gold particles labeled on vK138 appeared as spikes protruding radially from the virus particle, suggesting that the gold particles are longitudinally mobile. In contrast, the gold particles labeled on vK299 were imaged as islands of density, indicating that the gold particles are associated with latitudinal motion on a larger scale and only their "vibration center" is visible. K139 is located in a structural valley between large and small subunits, and only motion in a radial direction is permitted, while K299 is more on an "open field," allowing more freedom of movement (Figure 4B). The labeling of gold particles at designated locations demonstrates that the surface of the virus particle is selectively addressable.

The Environment of Lys Residues on the Capsid Surface

It is reasonable to suggest that the free amines (i.e., those not involved in salt links or hydrogen bonding) are more reactive than those restricted by existing interactions. The environments of the surface Lys residues are shown (Figure 5) based on the crystal structure of CPMV [4]. The three less reactive Lys residues, Lys182, Lys234, and Lys2199 (Figures 5B, 5C, and 5E, respectively), all interact with the surrounding residues either directly or via water molecules. Reactive Lys299 is fully exposed on the virus surface, with no neighboring residues close enough to interact with its amine groups (Figure 5D). Lys138 is the most reactive residue. However, it and three neighboring side chains interact with a water molecule (Figure 5A). In spite of these interactions, $N\epsilon$ of Lys138 has a high temperature factor when compared to the neighboring residues (Figure 5A). The reactivity of Lys138 is thus enigmatic in terms of the crystal structure, since the side chain has both interacting neighbors and high mobility.

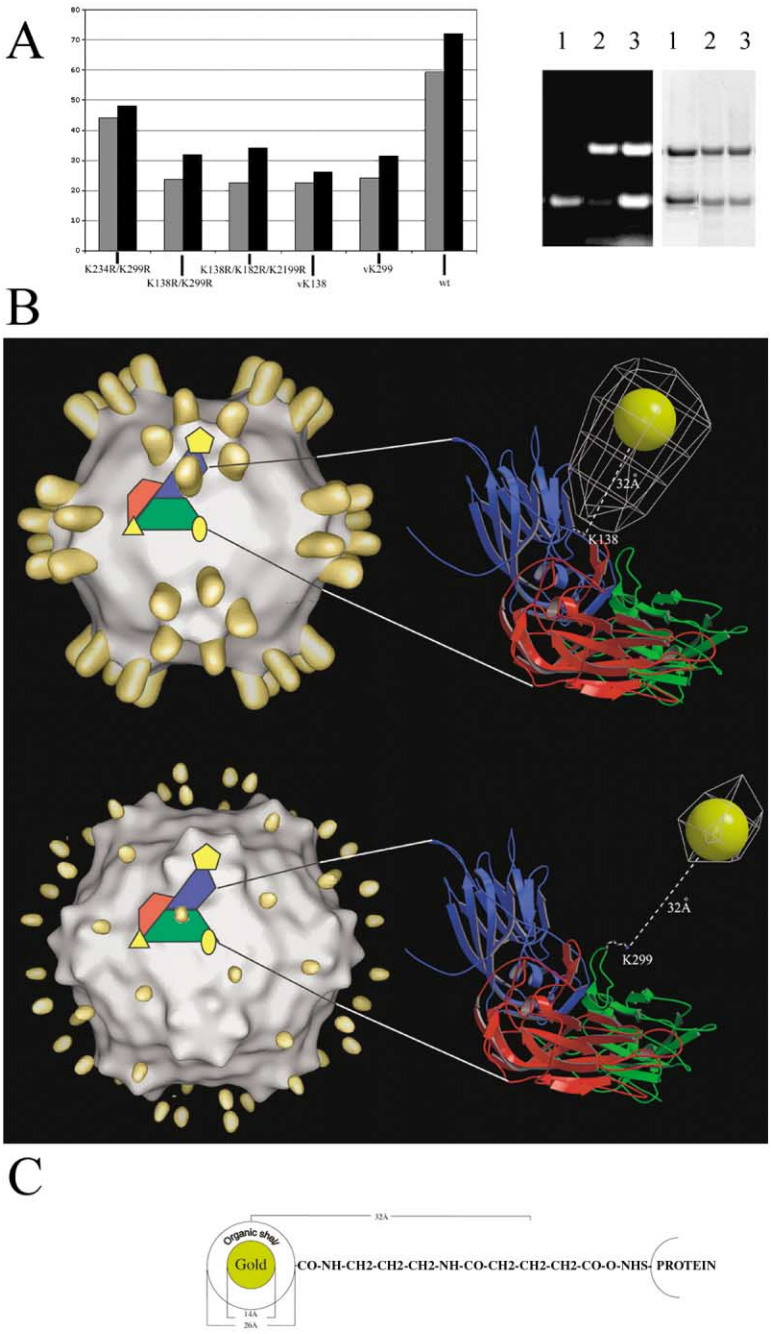

Figure 4. Relative Reactivity of Multiple Lys-Minus Mutants

(A) At left is the number of fluorescein molecules attached to the virus mutants modified with FITC (gray) and fluorescein NHS ester (black). On the right is SDS-PAGE analysis of FITC-modified Lys-minus mutants with unique Lys138 in the small and Lys299 in the large subunit of CPMV under forcing conditions. The SDS-PAGE gels were illuminated under UV (left) or stained with Coomassie blue (right). Lane 1, vK138; lane 2, vK29; lane 3, the WT CPMV as a control. The labeling to vK138 with FITC is exclusively limited to the S subunit, while labeling to vK299 is associated with the L subunit.

(B) Images of gold-decorated CPMV mutants as determined by cryo-electron microscopy and image reconstruction. On top is shown a cryo-EM image of NANOGOLD-labeled mutant vK138. The image is a composite of the native virus (gray) and difference map between the CPMV/gold conjugates and the native virus (gold). The asymmetric unit of the capsid and the symmetry operators are shown. The gold particles appear as spikes protruding from Lys138. Difference electron density, derived from vK138-gold conjugate, is superimposed with the ribbon diagram of the asymmetric unit of the virus capsid on the right. The stearic constraint restricts the movement of gold particles. The A domain is represented in blue, the B is shown in red, and the C is denoted in green. The gold particle is drawn as a yellow sphere with a diameter of 14 Å. The center of the gold particle to the Lys residue is 32 Å. At bottom is a cryo-EM Image of NANOGOLD/vK299 conjugate, similarly illustrated as for vK138 conjugate. The density corresponding to gold particles appears as islands, suggesting considerable latitudinal motion. As shown in the ribbon diagram, there is less constraint on the gold particles labeled at this site.

(C) The schematic representation of the linker arm distance of 32 Å between the center of the density for gold and the labeled lysine residues, which includes the sum of the size of the gold, the organic shell around the gold, and the length of the cross linker.

Significance

The inherent properties of virus particles, such as organized assembly, extensive exterior surface, enclosure of large internal space, and the propensity to form arrays, make them highly suitable as templates for creating functional nanomaterials with biomedical and pharmaceutical applications [15–19]. To exploit biological molecules as chemically reactive entities and assembly units, the ability to alter the constituent reactive groups or introduce unique functional groups makes these biological molecules addressable and, therefore, prospective templates in formation, assembly, and patterning of organic and inorganic molecules. CPMV, an icosahedral virus, has been demonstrated to be exceptionally useful in this regard [6–10]. We have previously shown the introduction of unique Cys residues that conferred thiol chemistry to the virus particles [6, 10]. Engineering of CPMV variants with uniquely reactive lysine residues provides an additional opportunity to employ amine-specific chemistry for covalent modification of the virus at those sites while retaining the ability to differentially address the cysteines through the use of thiol-specific reagents. Modification of viral capsids with NANOGOLD particles at unique lysine residues demonstrates the speci-

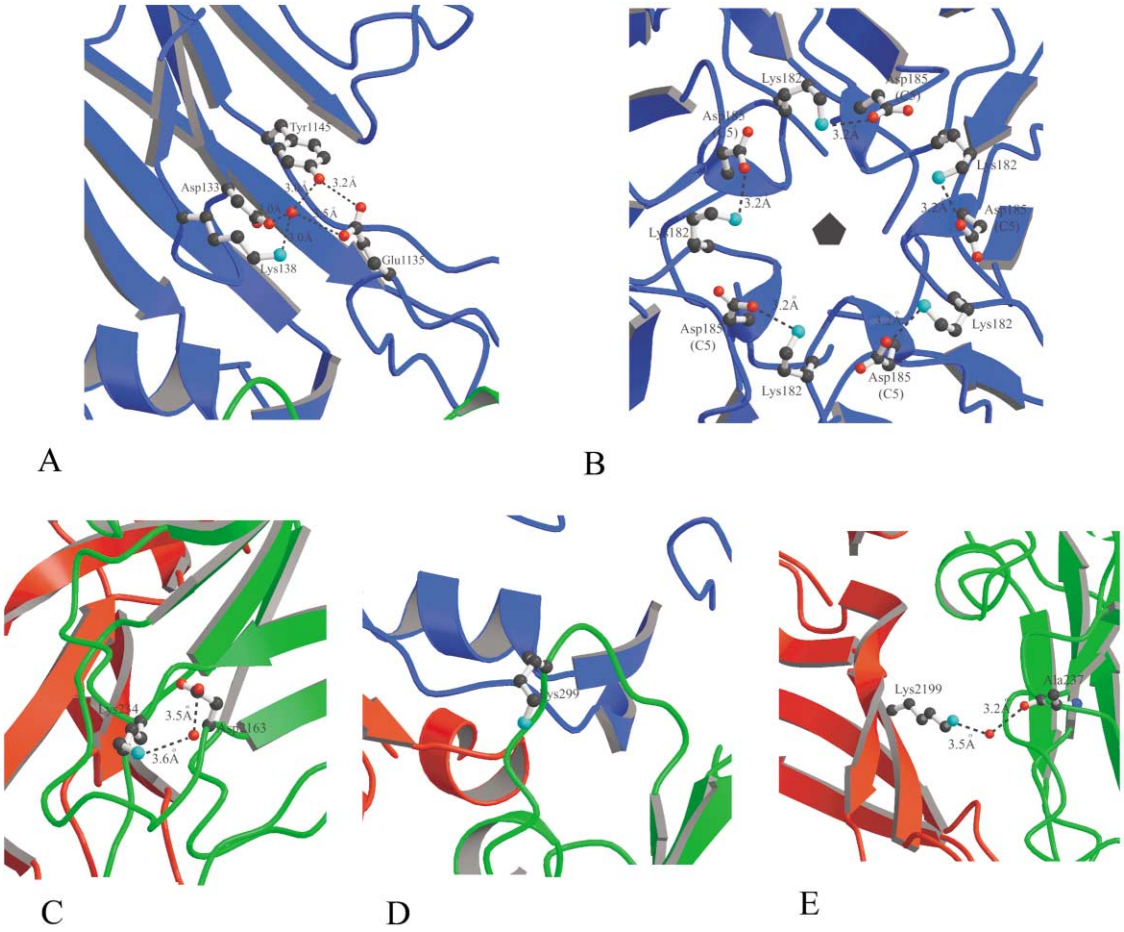

Figure 5. Environments of Surface Lys Residues

A domain is in blue, B domain is in red, and C domain is in green. Black spheres represent carbon atoms, red spheres represent oxygen atoms, and the cyan spheres represent nitrogen atoms.

(A) The amine group of Lys138 and three neighboring residues interact with a water molecule. However, the Nϵ of Lys138 has the highest B factor of 48.0. In comparison, the B factor of Oη of interacting Tyr1145 is 16.6, that for Oϵ1 of Glu1135 is 26.5, and 21.2 for Oσ1 of Asp133. It is possible that Nϵ of Lys138 can have more freedom for the attachment of fluorescein molecules, without the interruption of the interaction between the water and the other three residues.

(B) Nϵ of Lys182 interacts with 5-fold related Glu185. While the B factor for Nϵ of Lys182 is high (49.5), the B factor for Oϵ1 of Glu185 is also high. It is possible that both side chains can be mobile while maintaining the interaction. The pentagon represents the 5-fold axis.

(C) Lys234: Nϵ (B = 37.9) is in interaction with Asp163 via a water molecule.

(D) Lys299: the side chain is free of interaction and completely exposed (B = 51.44).

(E) Lys2199 (B = 33.92) interacts with the carbonyl oxygen of Ala237 via a water molecule.

ficity of labeling and the programmability of these building blocks on nanometer scale. The polyvalent presentation of a ligand of interest displayed icosahedrally on the viral surface coupled with the capability to employ different chemistries simultaneously enhances the use of these biological molecules for a wide array of applications and therefore should appeal to both chemists and biologists interested in using these viruses as biomaterials.

Experimental Procedures

Propagation of the Virus in Plants

The primary leaves of cowpea seedlings were mechanically inoculated with 10 μg each of cDNA plasmids encoding RNA1 (pCP1) and RNA2 (pCP2). The initial inoculum of native CPMV was extracted from infected leaves with 0.1 M potassium phosphate (pH 7.0) (phosphate buffer) 7 days post-infection. Typically, 50 plants were infected with the plant extract, and the symptomatic leaves were harvested after three weeks. The virus was isolated according to the standard protocol [3] with minor modifications.

Ultracentrifugation and Chromatography

Separation of CPMV from other materials can be achieved by ultracentrifugation for 3 hr at 42,000 rpm at 4°C in a 50.2Ti rotor (Beckman-Coulter). The viral supernatant was layered over 3 ml of 30% sucrose cushion and centrifuged. At the end of the run, a relatively clean glass-like virus pellet was obtained, which was briefly rinsed with phosphate buffer and resuspsended in the same buffer. Highly pure preparations were achieved by employing sedimentation velocity (sucrose) or equilibrium (cesium chloride) ultracentrifugation. The sucrose gradients were made with a 10% and 40% sucrose solution using Gradient Master (BIOCOMP). The virus was loaded on top of the gradient and centrifuged for 3 hr at 28,000 rpm in a SW41 rotor (Beckman-Coulter) at 4°C. The CsCl gradient was formed

by loading the centrifuge tube with 40% (w/w) CsCl mixed with the virus in phosphate buffer. The centrifugation was carried out at 38,000 rpm for 16 hr at room temperature in 50.2Ti rotor (Beckman-Coulter).

Purified viruses were analyzed by size exclusion (Superose6) and ion exchange (MonoQ) chromatography using the AKTA explorer (Amersham Pharmacia Biotech). The mutants eluted at 22 min with a flow rate of 0.4 ml/min in size exclusion chromatography, similar to the elution profile of the wild-type CPMV. Ion exchange chromatography was performed using 50 mM phosphate buffer (pH 7.0) as the low-salt buffer and 50 mM phosphate with 1.0 M NaCl (pH 7.0) as the high-salt eluant. The retention time of the Lys-minus mutants was similar to that of wild-type CPMV (38%–40% B, high-salt buffer).

Mutagenesis

Site-directed mutagenesis of pCP2 (coding for RNA2 of CPMV) to generate Lys-minus mutants was carried out based on established protocols [13]. Complementary oligonucleotides spanning the sequences around the substituted nucleotides (Lys to Arg) were synthesized (Sigma Genosys) and used for PCR amplification. The PCR product was ligated and transformed in *E. coli* cells using standard molecular biology methods. The clones obtained were verified by sequencing and used to transfect young cowpea seedlings as for the native virus. The primers used for the mutagenesis are as follows: K138R, F 5′-GACTTAATCAACGGCAGAATAACTCCTGTT-3′, R 5′-AACAGGAGTTATTCTGCCGTTGATTAAGTC-3′; K182R, F 5′-GGTGCTGGTGTCAGAAGAGCAGATTGG-3′, R 5′-CCAATCTGCTCTTCTGACACCAGCACC-3′; K234R, F 5′-GTTTTGTTGTCCAGGGCTATGGCTGGT-3′, R 5′-ACCAGCCATAGCCCTGGACAACAAAAC-3′; K299R, F 5′-GGTGTGAGGGGTAGGTATAGTACTGAT-3′, R 5′-ATCAGTACTATACCTACCCCTCACACC-3′; K2199R, F 5′-CGTTGGATGGGAAGATTGACTTTTCCC-3′, R 5′-GGGAAAAGTCAATCTTCCCATCCAACG-3′.

RNA Extraction and Analysis

Total RNA was extracted from primary and secondary leaves of the infected plants using Trizol (GIBCO-BRL). The cDNA fragments were generated by reverse transcription using virus-specific primer (5′-CCTAACTCTGCTTCGACT-3′) and MMLV Reverse Transcriptase (Invitrogen) and analyzed by PCR with a pair of primers (5′-GGAGAAAGTTTGAAATAC-3′ and 5′-CAATAACACATCACCACC-3′). The RT-PCR products were analyzed by electrophoresis on 3% agarose gels. A primer derived from the wild-type CPMV RNA2 sequence (5′-GGAGAAAGTTTGAAATAC-3′) was used for DNA sequencing.

Mutant Virus Purification

The Lys-minus mutants were purified using the procedure as native CPMV [3], except phosphate buffer used in the final suspension of the virus pellet was supplemented with 0.01% glycerol.

Chemical Derivatization of CPMV

Five milligrams of virus was incubated with 200× excess of fluorescein NHS ester or 1000× excess of FITC (Molecular Probes) in a solution mixture of 20% DMSO and 80% phosphate buffer at room temperature (pH 7.0) in a total reaction volume of 100 μl. The reactions were incubated for 2 hr at room temperature for fluorescein NHS ester, while the FITC reactions were continued for 18–24 hr. After the reaction, the excess dye molecules were removed by repeated rounds of ultracentrifugation on 10%–40% sucrose gradients. The fluorescent bands corresponding to the modified virus were collected and diluted with phosphate buffer. The derivatized virus was recovered by ultracentrifugation and analyzed by ion exchange and size exclusion chromatography. The amount of dye attached was determined by measuring the absorbance of dye modified virus samples at 495 nm with a spectrophotometer. Virus concentration was measured by determining the absorbance at 260 nm. The concentration of the virus at 0.1 mg/ml in the sample thickness of 1 cm corresponds to an O.D. reading of 0.8. Each data point was obtained from the average of three independent, parallel reactions, which were repeated at least three times. The typical variation was 5%–15%.

The amount of dye loading was increased by raising the pH of the labeling reaction to pH 8.5 in 0.1 M sodium bicarbonate with either NHS ester or FITC and extending the incubation time to 24 or 48 hr, respectively. These conditions were referred to as "forcing conditions" for virus labeling.

Labeling the Unique Lysine Mutants with NANOGOLD

Six nanomols of Monosulfo NHS NANOGOLD (Nanoprobes Inc.) was dissolved in 90 μl of 0.1 M sodium bicarbonate buffer (pH 8.0) and mixed with 10 μl (60 μg) of unique lysine mutant (vK138 or vK299). The reaction was incubated for 1 hr at room temperature followed by overnight incubation at 4°C. Following incubation, the excess gold was removed by passing the reaction mix over a Superose6 size exclusion column. The fractions containing the virus/gold conjugates were collected, concentrated to 1 mg/ml, and used for cryo electron microscopy.

Cryo-Electron Microscopy and Image Reconstruction

CPMV/gold conjugates were applied to glow discharged quantifoil EM grids and frozen under liquid nitrogen. The cryogenic temperature was maintained at −184 ± 2°C in a Gatan Cryo-transfer-holder for image requisition. The Philips CM120 transmission electron microscope was operated at 100 KV and under minimum dose conditions of about 15–10 electrons/Å^2.

Micrographs at 60,000× magnification were recorded with the defocus of the objective lens at between 0.6 and 1.7 μm. Selected micrographs were digitized to a final pixel size of 3.5 Å on the object scale with a Zeiss imaging scanner. For the vK38 and vK299 gold conjugates, a total of 2439 and 931 particles were manually selected, respectively, using the program Boxer [20]. The image reconstruction was performed with the SPIDER/WEB software package [21], using the native CPMV structure as the starting model. Twenty cycles of refinement were performed at 1.0 angular intervals, then repeated with 0.5 angular steps for increased accuracy. The final resolution was 25 Å and 26 Å, respectively, estimated by Fourier Shell correlation with a cut-off of 0.5. The electron density maps were normalized, taking into the account their average density and variability. Difference maps were calculated by subtracting the native CPMV reference volume. The atomic models of CPMV and gold particles were fit into the electron density maps manually by using the program O [22]. The images were rendered using the programs Bobscript [23] and Chimera [24].

Acknowledgments

Helpful discussions with Drs. Kelly Lee and Liang Tang are greatly appreciated. The authors thank Dr. George Lomonosoff for providing the infectious CPMV cDNA clones. Funding from NIH (R01 EBB00432-02 to J.E.J.) and the Naval Research Laboratory grants (N00014-00-1-0671 to J.E.J. and N00014-03-1-0632 to T.L.) is also acknowledged.

Received: September 3, 2003
Revised: March 25, 2004
Accepted: April 21, 2004
Published: June 25, 2004

References

1. Lomonossoff, G.P., and Johnson, J.E. (1991). The synthesis and structure of comovirus capsids. Prog. Biophys. Mol. Biol. *55*, 107–137.
2. Lin, T., and Johnson, J.E. (2003). Structures of picorna like plant viruses: Implications and applications. Adv. Virus Res. *62*, 167–239.
3. Wellink, J. (1998). Comovirus isolation and RNA extraction. In Plant Virology Protocols, G. Foster and S. Taylor, eds. (Totowa, NJ: Humana Press), p. 205.
4. Lin, T., Chen, Z., Usha, R., Dai, J.-B., Schmidt, T., and Johnson, J.E. (1999). The refined crystal structure of cowpea mosaic virus at 2.8-Å resolution. Virology *265*, 20–34.
5. Dessens, J.T., and Lomonossoff, G.P. (1993). Cauliflower mosaic virus 35s promoter controlled DNA copies of cowpea mosaic virus RNAs are infectious on plants. J. Gen. Virol. *74*, 889–892.
6. Wang, Q., Lin, T., Tang, L., Johnson, J.E., and Finn, M.G. (2002).

Icosahedral virus particles as addressable nanoscale building blocks. Angew. Chem. Int. Ed. Engl. *41*, 459–462.
7. Chatterji, A., Burns, L.L., Taylor, S.S., Lomonossoff, G.P., Johnson, J.E., Lin, T., and Porta, C. Cowpea mosaic virus: from the presentation of antigenic peptides to the display of active biomaterials. Intervirology *45*, 362–370.
8. Cheung, C.L., Camarero, J.A., Woods, B.W., Lin, T., Johnson, J.E., and De Yoreo, J.J. (2003). Fabrication of virus assembled nanostructures with chemoselective linkers by scanning probe nanolithography. J. Am. Chem. Soc. *125*, 6848–6849.
9. Raja, K.S., Wang, Q., Gonzales, M.J., Manchester, M., Johnson, J.E., and Finn, M.G. (2003). Hybrid virus-polymer materials. 1. Synthesis and properties of PEG-decorated Cowpea mosaic virus. Biomacromolecules *4*, 472–476.
10. Wang, Q., Lin, T., Johnson, J.E., and Finn, M.G. (2002). Natural supramolecular building blocks: cysteine-added mutants of Cowpea mosaic virus. Chem. Biol. *9*, 813–819.
11. Wang, Q., Kaltgrad, E., Lin, T., Johnson, J.E., and Finn, M.G. (2002). Natural supramolecular building blocks: wild-type Cowpea mosaic virus. Chem. Biol. *9*, 805–811.
12. Hermonson, G.T. (1996). Bioconjugate Techniques (San Diego, CA: Academic Press).
13. Horton, R.M. (1994). *In vitro* recombination and mutagenesis of DNA. Methods Mol. Biol. *67*, 141–150.
14. Kraulis, P.J. (1991). MOLSCRIPT: a program to produce both detailed and schematic plots of protein structures. J. Appl. Crystallogr. *24*, 946–950.
15. Douglas, T., and Young, M. (1999). Virus particles as templates for nanophase material synthesis. Adv. Mater. *11*, 679–681.
16. Shenton, W., Douglas, T., Young, M., Stubbs, G., and Mann, S. (1999). Inorganic-organic nanotube composites from template mineralization of tobacco mosaic virus. Adv. Mater. *11*, 253–256.
17. Douglas, T. (2003). A bright bio-inspired future. Science *299*, 1192–1193.
18. Gillitzer, E., Willits, D., Young, M., and Douglas, T. (2002). Chemical modification of a viral cage for multivalent presentation. Chem. Commun. (Camb.) *20*, 2390–2391.
19. Peabody, D.S. (2003). A viral platform for chemical modification and multivalent display. J. Nanobiotechnology *1*, 5–12.
20. Ludtke, S.J., Baldwin, P.R., and Chiu, W. (1999). EMAN: semiautomated software for high-resolution single-particle reconstructions. J. Struct. Biol. *128*, 82–97.
21. Frank, J., Radermacher, M., Penczek, P., Zhu, J., Li, Y., Ladjadj, M., and Leith, A. (1996). SPIDER and WEB: processing and visualization of images in 3D electron microscopy and related fields. J. Struct. Biol. *116*, 190–199.
22. Jones, T.A., Zou, J. Y, Cowan, S.W., and Kjeldgaard. (1991). Improved methods for building protein models in electron density maps and the location of errors in these models. Acta Crystallogr. A. *47*, 110–119.
23. Esnouf, R.M. (1997). An extensively modified version of MolScript that includes greatly enhanced coloring capabilities. J. Mol. Graph. Model. *15*, 132–134, 112–113.
24. Sanner, M.F., Olson, A.J., and Spehner, J.C. (1996). Reduced surface: an efficient way to compute molecular surfaces. Biopolymers *38*, 305–320.